Microchemical Journal 155 (2020) 104756

Contents lists available at ScienceDirect

Microchemical Journal

journal homepage: www.elsevier.com/locate/microc

Characterization of model samples simulating degradation processes induced by iron and sulfur species on waterlogged wood

Mathilde Monachon[a], Magdalena Albelda-Berenguer[a], Charlène Pelé[b], Emilie Cornet[c], Elodie Guilminot[b], Céline Rémazeilles[d], Edith Joseph[a,c,*]

[a] Laboratory of Technologies for Heritage Materials (LATHEMA), University of Neuchâtel, Avenue de Bellevaux 51, 2000 Neuchâtel, Switzerland
[b] Arc'Antique, laboratoire de conservation, de restauration et de recherches, 26 rue de la Haute Forêt, 44300 Nantes, France
[c] Haute Ecole Arc Conservation-restauration, HES-SO, Espace de l'Europe 11, 2000 Neuchâtel, Switzerland
[d] Laboratoire des Sciences de l'Ingénieur pour l'Environnement (LaSIE), UMR CNRS 7356, Avenue Michel Crépeau, 17042 La Rochelle, France

ARTICLE INFO

Keywords:
Model samples
Waterlogged archaeological wood
Raman spectroscopy
ATR-FTIR spectroscopy
Chemometrics

ABSTRACT

Reduced iron and sulfur species accumulated within waterlogged archaeological wood artefacts during their burial time. Oxygen exposure of the artefacts during recovery leads to acidification and salts precipitation, which causes irreversible physical and chemical damages. Prior to accurately evaluating novel extraction methods, the procedures for creating analogous samples were evaluated for efficacy. Waterlogged wood analogues provide access to a whole set of homogeneous and sacrificial samples that replicate characteristics of waterlogged archaeological wood in terms of content degradation and the presence of reduced iron and sulfur species. In this study, we evaluated the preparation of model samples from fresh balsa wood artificially contaminated with reduced iron and sulfur species. Wood degradation and the formation of reduced iron and sulfur species were assessed by Fourier Transformed Infrared (FTIR) and Raman spectroscopies and validated through statistic methods, such as Principal Component Analysis (PCA). Among the three impregnation protocols investigated, one method appeared to be the most effective in term of iron sulfide formation, especially partially oxidized mackinawite $Fe_{1-x}S$. The selected protocol proved reproducible and efficient on both fresh balsa and Neolithic oak samples. From these observations confirmed by the PCA analyses on spectroscopic dataset, a suitable method to model waterlogged archaeological wood was established.

1. Introduction

1.1. Waterlogged wood degradation

Waterlogged archaeological wooden artefacts found in anoxic environments can suffer from salt efflorescence and acidification issues, even after consolidation treatments have been undertaken. Due to the low oxygen concentration, darkness and low water temperatures found in anaerobic conditions, bacteria are the main degradation agents. For instance, sulfate-reducing bacteria (SRB) can metabolize organic matter, such as carbohydrates and polysaccharides, to produce hydrogen sulfide (H_2S), which diffuses into the wood. The presence of iron, from either the burial sites or the objects themselves, contributes to the wood degradation. Soluble iron (II) may interact with H_2S to produce iron sulfides that then accumulate within the wood vessels [1]. Iron sulfides alter the color of the waterlogged wooden artefacts [2,3]. These compounds are detected in most waterlogged archaeological wood objects, such as the *Vasa* or the *Mary Rose* warships but also in corrosion layers of archaeological iron artefacts [4]. Pyrite (FeS_2) is the most documented phase in literature; however other iron sulfides such as mackinawite (FeS) or greigite (Fe_3S_4) are reported as well [5,6].

Throughout the recovery and subsequent modifications of environmental conditions, archaeological objects suffer from the oxidation of these compounds due to exposure to different oxygen concentrations and relative humidity rates. In particular, iron sulfides are converted into sulfuric acid and/or salts efflorescence, resulting in irreversible chemical and mechanical damages [1]. Acid hydrolysis leads to cellulosic degradation that weakens the strength of the wood structure. The conversion of reduced species into ferric oxyhydroxides and/or iron sulfates from the oxidation process can collapse the object's cellular structure due to volume expansion [1,7,8].

Moreover, iron ions can catalyze several chemical reactions that are

* Corresponding author at: Laboratory of Technologies for Heritage Materials (LATHEMA), University of Neuchâtel, Avenue de Bellevaux 51, 2000 Neuchâtel, Switzerland and Haute Ecole Arc Conservation-restauration, HES-SO, Espace de l'Europe 11, 2000 Neuchâtel, Switzerland.
E-mail addresses: edith.joseph@unine.ch, edith.joseph@he-arc.ch (E. Joseph).

https://doi.org/10.1016/j.microc.2020.104756
Received 30 August 2019; Received in revised form 19 February 2020; Accepted 20 February 2020
Available online 21 February 2020

harmful to the wood structure [3]. Fe (II) ions can initiate and catalyze the cellulosic content degradation and oxidation by Fenton-type reaction [3,7,9]. In addition, sulfuric acid may form from the oxidation of sulfur compounds by Fe (II) ions.

1.2. Conservation treatments

Different consolidation methods are used to preserve waterlogged wooden objects after their recovery. Among them, polyethylene glycol (PEG) is widely used. It was initially developed for the *Vasa* warship in Sweden [8]. The Swedish warship was consolidated by spraying an aqueous solution of PEG for 17 years [9]. While this method maintains the wood shape against distortion and deterioration, studies have demonstrated that iron parts still present in the wooden matrix corrode in contact with PEG. The formation of Fe (II) ions induce the decomposition of the PEG molecules, thus inhibiting its consolidation role and preventing the long-term preservation of the waterlogged wood artefacts [3].

The investigations carried out on important waterlogged wood items, such as the *Vasa* or the *Mary Rose*, estimate a total sulfur content of 2 to 3 tons as well as 5 tons of iron for the *Vasa* [3,9,11]. It is important to extract iron and sulfur species to minimize their impact on the preservation of the waterlogged wood. These studies also demonstrated that these species are concentrated within the two first centimeters of the wood substrate. Post-consolidation extraction methods were employed for the neutralization of sulfuric acid. Alkaline baths or ammonia gas present short-term effectiveness, but cause holocellulose degradation in the long-term [12]. In addition, the use of alkaline nanoparticles provided efficient long-term neutralization, but proved potentially toxic and difficult to remove potential sub-products [13]. Strong oxidants and chelating agents were also used for iron extraction, such as EDMA (ethylenediiminobis (2-hydroxy-4-methyl-phenyl) acetic acid) [3]. Even though the EDMA-based iron extractions were effective, the objects developed a red hue and swelling after treatment. Moreover, the long-term effects remain unknown. Due to the concerns and issues surrounding PEG treatments, Tahira et al. [14] and Broda et al. [15] tested polysaccharides and methyltrimethoxysilane, respectively. With encouraging first results, these new methods represent interesting alternatives to current consolidation agents. The development of extraction methods applied before any consolidation treatments has also been proposed recently with either chemicals or microorganism-based treatments [2, 16].

1.3. Model samples

The purpose of modeling waterlogged wood degradation is to obtain a representative set of wood samples that replicate the characteristics of archaeological waterlogged wood, meaning a low carbohydrates content (wood fraction composed of cellulose and hemicellulose and defined as holocellulose) and the presence of iron sulfides (i.e. greigite, pyrite and mackinawite). As explained in Section 1.1, these two criteria are reported on real waterlogged wood samples. The preparation of similar model samples has been reported in previous studies for the assessment of extraction methods; however, some of these approaches require specific equipment (i.e., H_2S gas supply) and have complicated regulations to comply with. Thus, these methods are difficult to implement and ill-suited for some laboratories [8]. Iron exctraction methods were investigated through modeling of samples artificially contaminated with iron species [17, 18]. These iron-focused methods were also performed with fresh oak wood [8, 9].

This article focuses on the preparation of model samples with fresh balsa wood. The application of chemometrics established clear parameters for a valid protocol, which will be employed to contaminate wood artificially with iron sulfides and model archaeological waterlogged wood. Within this study, three different impregnation protocols were evaluated for their efficiency in terms of wood degradation and iron sulfides formation through colorimetry, shrinkage and spectroscopic analyses.

2. Material and methods

2.1. Preparation of model samples

2.1.1. Wood samples

Balsa wood (*Ochroma pyramidale*) was purchased in a 1-meter listel (Coop Brico + Loisir®) and cut in 2 × 2 × 2 cm^3 samples presenting radial (Rd), transversal (Tv) and tangential (Tg) sections. This wood specie was selected as it presents a similar porosity to waterlogged archaeological wood, allowing an easier degradation of the carbohydrates content. The chemical composition of balsa showed that balsa wood is composed of 40–45% of cellulose, 25% of lignin and 23–26% of hemicellulose, for dry-wood [19]. In particular, glucomannan (acetyl groups) and xylan are the main component of hemicellulose and their fraction are of 2–5% and 21%, respectively. Moreover, its light color can facilitate monitoring the color variation of the samples when artificially impregnated with iron sulfides. Each impregnation protocol (IP) was assessed in triplicates. The samples were weighted and distributed into different sample groups based on mass to have homogeneous representative experimental sets and significant results. Two samples were characterized, and another sample was poured in deaerated deionized water and kept at 4 °C in a fridge as a reference sample.

2.1.2. Impregnation protocols

All chemical reagents used for the different impregnation protocols were of analytical grade. Three artificial contamination protocols (IP1, IP2 and IP3) were selected from literature and are summarized in Table 1. Before impregnation, the cubes were pre-immersed for one week in deionized water under vacuum (600 mbars). After impregnation, the samples were wrapped in plastic film and stored at 4 °C in Ziploc bags® filled with deaerated water to prevent from oxidation until characterization was completed. The archaeological nails employed in IP2, were excavated from chalky soil in the Champagne region, France, dating from the late Roman period (3rd century A.D). They present a corrosion layer composed of a mixture of goethite (α-FeOOH) and lepidocrocite (γ-FeOOH) identified by Raman spectroscopy.

2.1.3. Round robin test

To validate the preparation of model samples, LATHEMA (Neuchâtel, Switzerland) and Arc'Antique (Nantes, France) laboratories worked in parallel to evaluate the same IP using the same parameters (i.e., wood degradation and the formation iron sulfides). The results obtained were gathered and compared to evaluate the feasibility and reproducibility of the selected artificial impregnation protocol.

Table 1
Parameters used for the impregnation of fresh balsa wood, modelling archaeological waterlogged wood

	Impregnation protocol	*Reference*
IP1	• 4 h immersion in 800 ml of iron(II) chloride tetrahydrate ($FeCl_2{\cdot}4H_2O$) 0.5 M under vacuum (600 mbars) • overnight drying • 4 h immersion in 800 ml of sodium sulfide nonahydrate ($Na_2S{\cdot}9H_2O$) 0.5 M under vacuum (600 mbars)	[16]
IP2	• immersion in artificial sea water in presence of archaeological terrestrial nails • treatment time of 18 or 60 days • optional vacuum (600 mbars)	[45]
IP3	• 8 h immersion in 800 ml of $Na_2S{\cdot}9H_2O$) 0.12 M and 800 ml of $FeCl_2{\cdot}4H_2O$ 0.09 M	[48]

2.2. Analytical methods

2.2.1. Colorimetry

Colorimetry measurement was investigated to determine the variation of samples appearance. This method is a fast screening approach to identify potential chemical changes on the sample surfaces through the quantification of color shifts. This type of assessment provides complementary information to other forms of characterization. A Minolta CM-508D spectrophotometer was used for the color measurements, with the following parameters: Specular Component Included (SCI), Illuminant D65 (daylight containing UV component, color T 6504 K), d/8° geometry, 10° observer, measurement area diameter 10 mm, illumination with Xe flash light source 100% UV containing all UV components or 0% UV containing no UV components, CIELab 1976 color space (EN ISO 11664-5:2016). On each sample, one measurement was recorded per cube face through the plastic film.

2.2.2. Raman spectroscopy

The iron minerals formed during the impregnation protocols were determined by Raman spectroscopy. Raman spectroscopy is widely used in the field of conservation-restoration as a non-invasive and non-destructive method, especially for waterlogged wood [20]. Additionally, the main iron corrosion products, sulfides or oxides, are well documented in the literature [20, 22]. A Jobin Yvon Horiba™ spectrophotometer was employed for the measurements coupled with an Olympus BX41 microscope. Spectra were recorded at a wavelength of 632 nm, a hole of 1000 µm, a slit of 100 µm, 100–1500 cm^{-1} range, 50xLWD objective, and acquisition with 10 accumulations of 5 s. A 25% filter (9.9 mW) was applied to avoid the degradation of thermosensitive compounds under the laser beam. Four spectra per face were recorded according to a specific mask (Fig. 1). A total of 24 spectra per sample was obtained. The spectra were analysed with LabSpec® software (automatic baseline correction). Reference spectra were used to identify the compounds formed. Samples were immersed in their stock solution to allow an increase in laser power and to obtain a good signal-to-noise ratio.

2.2.3. ATR-FTIR spectroscopy

Fourier Transformed Infrared spectroscopy was used to evaluate wood degradation. ATR-FTIR spectroscopy is largely used in the field of waterlogged wood conservation and preservation as a fast, non-invasive, and non-destructive method to evaluate the state of degradation [17,23,24]. A Nicolet iS5 Thermo Fisher™ was employed with the following parameters: range 400–4000 cm^{-1}, a spectral resolution of 4 cm^{-1}, and 16 scans. The measurements were performed in ATR (Attenuated Total Reflectance) mode using a diamond ATR crystal without any sample preparation (ID5 ATR accessory). Background was recorded in air. Four spectra were recorded on the wood surface and on half-sectioned (samples divide into two pieces along Tv section) samples using the same mask as for Raman measurements (Fig. 1). A total of 24 spectra per sample was obtained. The spectra were analysed with Thermo® OMNIC software. Baseline correction and frequency normalization were applied to the spectra. In particular, wood degradation was evaluated by calculating the ratio H/L = I(1158)/I(1506) with I(1158) and I(1506) being the height of the vibrational bands at 1158 and 1506 cm^{-1}, assigned to holocellulose and lignin respectively [25–28]. Ratios, before and after impregnation, were compared to ascertain related carbohydrates content degradation.

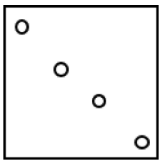

Fig. 1. Mask used fort the Raman and ATR-FTIR measurements

2.2.4. Physical shrinkage

Before and after impregnation, some samples were placed in oven at 100 °C and dried until a constant weight was obtained. The radial (Rd), tangential (Tg) and transversal (Tv) wood sections were then measured to estimate the eventual shrinkage of wood observed during impregnation.

2.2.5. Waterlogged archaeological wood samples

In parallel, Neolithic oak wood, recovered from Biel lake and dated from -2700 BC, was impregnated with the IP1 protocol. The same analytical protocol was applied to compare the results of the artificially impregnated fresh balsa samples with waterlogged archaeological wood objects contaminated with iron and sulfur species as described in the literature.

2.3. Data analysis

Modeling was validated using chemometrics. Exploratory data analysis was performed by principal component analysis (PCA). This statistical method was used to differentiate and cluster data, so the most efficient impregnation protocol can be determined. All the statistical analyses were carried out with open source software Rstudio (https://www.rstudio.com/). ATR-FTIR ratios and mean values of color and shrinkage measurements were used for the analysis. Concerning Raman, a contingency table was used with value 1 if reduced sulfur species identified and 0 if not. Then, all spectra from the different impregnation protocols were compiled in Rstudio, and PCA analysis was carried out. Closer examination of the loadings and of which frequency contributes more to each principal component (PC) was performed.

3. Results

3.1. Colorimetric measurements

After impregnation, the first observations showed that IP1 and IP3 samples presented a dark hue while IP2 samples displayed a brownish hue (Fig. 2 A). This observation suggests that different compounds may have formed according to the IP employed. In particular for IP2, similar results were obtained regardless of the treatment time (18 or 60 days) set or the application of vacuum conditions (yes or no) (see Table 1). IP2 samples immersed for 18 days gained a darker hue only in the areas where nails are present. When vacuum conditions were also applied, the wood became darker on the surface but not within the samples' core. With a longer impregnation time (60 days) the wood turned darker on the surface and few areas of its core remained unchanged. Regarding the impregnated Neolithic oak samples, the appearance of the samples was not altered respect to the recovered wood with $\Delta E = 3.01 (\pm 1.19)$. Only the results for IP2 applied for 60 days will be discussed further.

The colorimetric coordinates obtained in the CIELab color space verified that all impregnation protocols altered the appearance of the samples. In terms of brightness (L*), IP1 and IP3 resulted in the darkest hue with values of 25.71 (± 0.8) and 28.85 (± 1.3), while IP2 samples became less darkened (41.18 ± 0.8). For comparison, balsa wood before impregnation at t_0 has L* = 70.24 ± 0.9 (Fig. 2 B). The brightness L* of impregnated Neolithic oak slightly decreased after IP1, from 28.30 (± 0.9) to 25.51 (± 0.3). IP1 and IP3 have similar a* and b* colorimetric coordinates, while IP2 and t_0 sample values are located in a diametrically opposed zone. The coordinates for a* and b* obtained for Neolithic oak samples scarcely variated and gathered with the one of fresh balsa IP1. A minor data dispersion was observed for IP1.

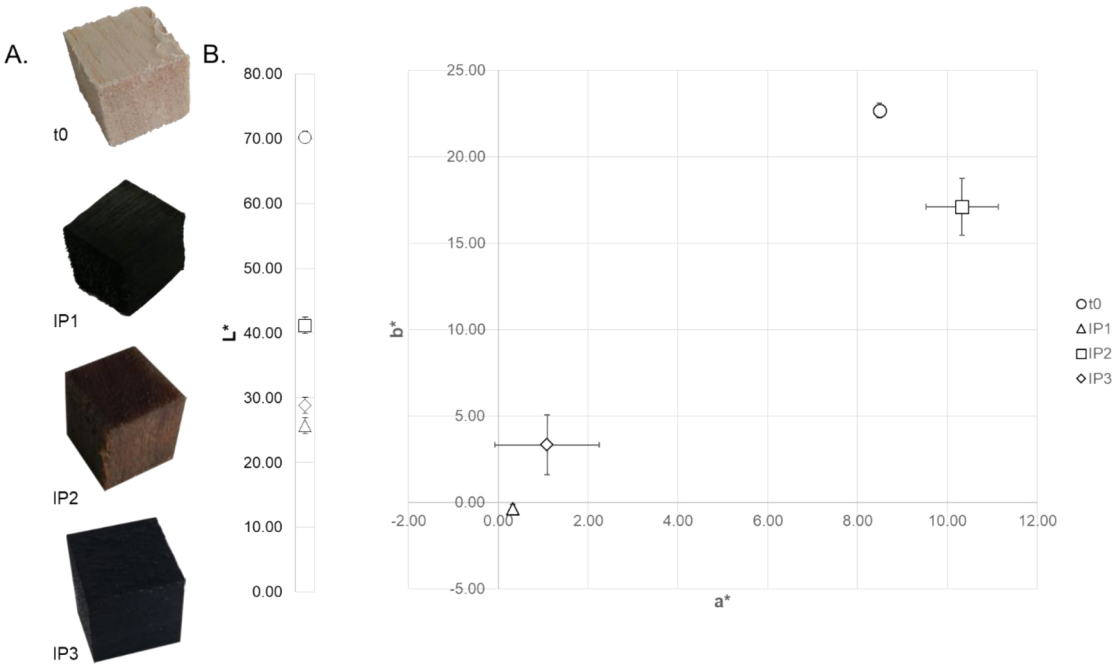

Fig. 2. A. Visual aspect of the balsa samples before impregnation (t0) and after each impregnation protocol (IP1, IP2 and IP3). B. Colorimetric plots in the CIELab color space before (t0 ○) and after impregnation (IP1 Δ, IP2 □, IP3 ◊)

3.2. Raman spectroscopy

Raman analyses were carried out on the samples' surface and core to identify the compounds formed during impregnation and to evaluate their depth of penetration in wood. As suggested by visual observations, different minerals were detected according to the impregnation protocol employed.

For both IP1 and IP3 samples, iron sulfides and sulfur compounds were identified. Mackinawite was detected on IP1 samples surface as partially oxidized mackinawite ($Fe_{1-x}S$) with characteristic vibrational bands at 214, 247 and 303 cm^{-1} [29] (Fig. 3 B). In addition, the vibrational band around 362 cm^{-1} was attributed to greigite (Fe_3S_4) and those at 150, 220 and 473 cm^{-1} to mineral sulfur α-S_8 [30]. These compounds were observed on both fresh and Neolithic samples. IP3 samples spectra mainly identified sulfur (α-S_8). Although a few spectra showed bands in the 350–360 cm^{-1} range, suggesting the presence of Fe_3S_4 (Fig. 3 B). For IP2 samples, iron oxides were identified as lepidocrocite (γ-FeOOH) with its characteristic vibrational bands at 252 and 380 cm^{-1} [31], (Fig. 3 B). On half-sectioned samples, the same compounds were identified within the first millimeters (Fig. 3 A).

3.3. ATR-FTIR spectroscopy

The degradation of the carbohydrates content was then evaluated (Fig. 3 C). Differences can be observed among the ATR-FTIR spectra before and after water pre-immersion but also after the impregnation protocols.

The first comparison of balsa samples was done between fresh and water pre-immersed under vacuum. The spectra of balsa wood with water pre-immersion showed shoulders at 897 and 1203 cm^{-1}. These bands were assigned to C—H deformation and OH plane deformation in cellulose and xylan (a component of carbohydrates in hemicellulose) [17]. These spectra also showed a band at 1650 cm^{-1} attributed to the H—O—H deformation of adsorbed water [17]. The band at 1128 cm^{-1} was assigned to aromatic skeleton; however C—O asymmetric stretching in cellulose slightly decreased in intensity after water pre-immersion [26]. First derivatives analyses carried out on the spectra highlighted those changes. Shoulders at these wavenumbers were observed by applying the 1st derivative to the fresh balsa spectrum except for the pre-immersed samples.

After impregnation, IP1 spectra presented a strong decrease in intensity at 1233 cm^{-1} attributed to both holocellulose and lignin wood contents [24,32] and at 1738 cm^{-1} (unconjugated C═O asymmetric stretching of acetyl and carbonyl groups in hemicellulose). The relative intensity of the bands at 1203 and 1318 cm^{-1} corresponding to cellulose increased slightly [33,34]. Whereas, the IP2 spectra were similar to those obtained after water pre-immersion. In this case, the band at 1738 cm^{-1} lost intensity and the band at 1590 cm^{-1}, attributed to aromatic skeletal and C═O stretching vibrations in lignin was absent [17]. The IP3 spectra were quite similar to the IP2 spectra, but two additional weak bands were observed at 1537 and 1550 cm^{-1}.

The spectra of Neolithic oak samples displayed a strong vibrational band at 1650 cm^{-1}, similar to those observed in the water pre-immersed balsa samples. However, the intensities of vibrational bands at 1034 and 1059 cm^{-1} were less intense on Neolithic oak. These bands were assigned to the C—O stretching of holocellulose and lignin (Fig. 3). In both spectra, before and after IP1, the bands at 1462 and 1506 cm^{-1} attributed to CH deformation and C═C stretch in lignin were more intense than the bands assigned to holocellulose.

To ascertain which wood fraction was degraded during impregnation, a ratio holocellulose/lignin (H/L) was calculated according to Dobrică et al. [25] and Macchioni et al. [27,28]. Similar values were obtained at the sample's surface and core (Table 2). In addition, the calculated H/L ratio confirmed that water immersion affected the wood's composition as values fresh to water pre-immersed balsa decreased from 2.67(± 0.37) to 1.45(± 0.17) between fresh and water pre-immersed balsa. While the ratios calculated after IP1 and IP3 impregnation decreased, the IP2 samples showed an increase of the H/L ratio. In the Neolithic wood samples, the H/L ratio before IP1 was higher than the one of fresh balsa with a value of 6.21 (± 2). After IP1, the ratio decreased to a value of 0.74 (± 0.09).

3.4. Shrinkage

Complementary measurements were performed on the samples to evaluate wood degradation. Wood shrinkage denotes a loss of size as

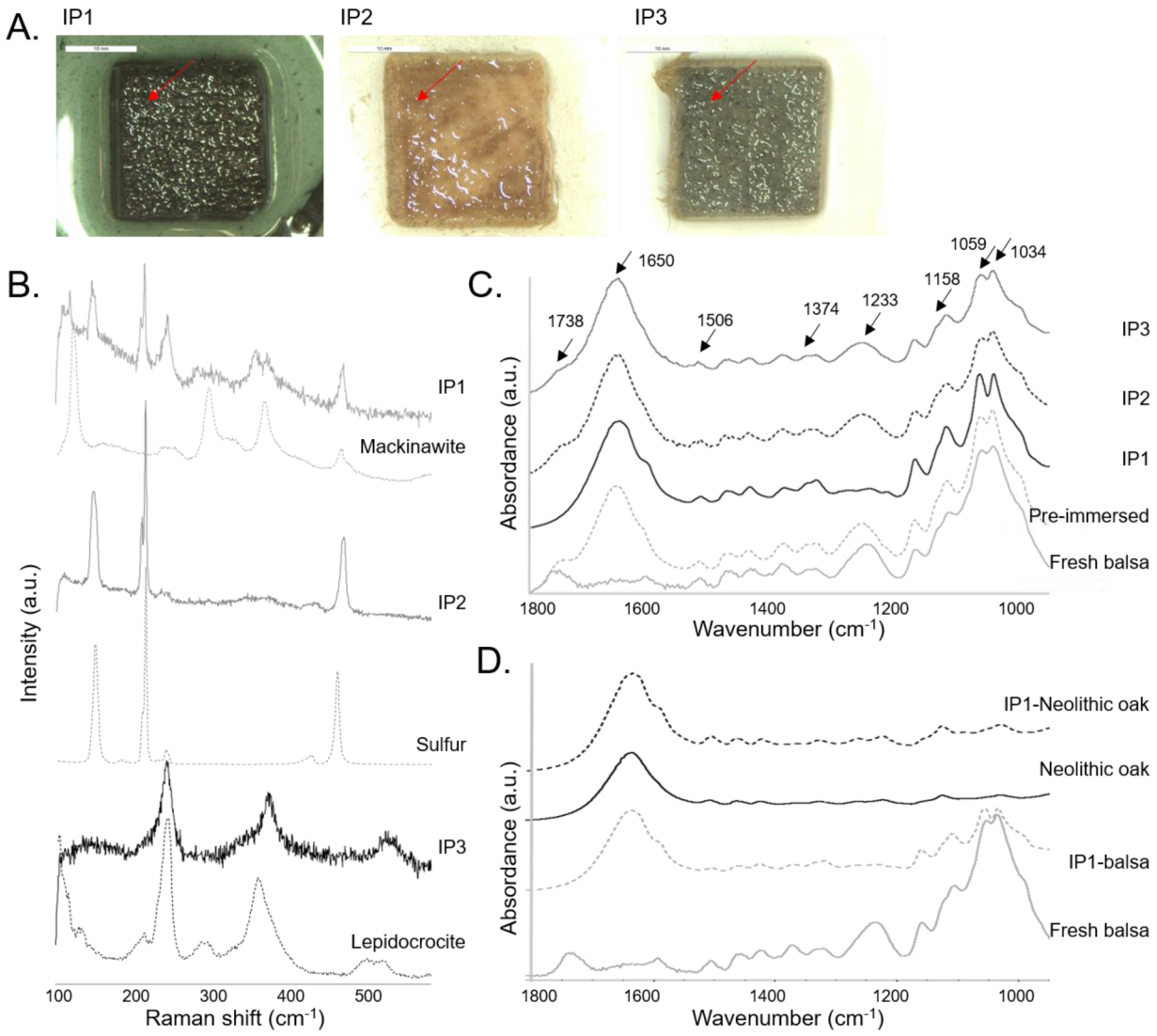

Fig. 3. A. Visual of transversal cut sections after impregnation protocols with spectroscopic measurements area indicated by red arrows. B. Representative Raman spectra obtained for IP1, IP2 and IP3 balsa samples with reference spectra of mackinawite, sulfur and lepidocrocite. C. Representative ATR-FTIR spectra of fresh (—), pre-immersed (—) and impregnated balsa samples (IP1 —, IP2 —, IP3 ••••••) with wood characteristic vibrational bands. D. Representative ATR-FTIR spectra of fresh (—) and IP1 (—) balsa samples as well as recovered (—) and impregnated (—) Neolithic oak samples.

well as a loss of strength of the wood. The length variation of the radial (Rd), tangential (Tg) and transversal (Tv) wood sections were calculated, and results are reported in Table 2. First observations showed that IP2 and IP3 samples did not shrink or very slightly after oven drying, especially the radial section (Rd). In contrast, IP1 samples showed length variation for all wood sections. IP1 samples collapsed during drying. Oven-dried Neolithic samples presented a higher shrinkage than fresh wood samples with length variation of ΔTv = 13.42 (± 0.61), ΔTg = 13.42 (± 0.42) and ΔRd = 8.17 (± 3.13). The shrinkage among the Rd sections for both fresh balsa (± 0.96) and Neolithic oak (± 0.61) was in the same range for IP1 samples.

3.5. Round Robin test

Both laboratories obtained similar results regarding the sample

Table 2
Evaluation of the wood content degradation by ATR-FTIR spectroscopy and shrinkage measurements on balsa and Neolithic oak wood, with mean value of H/L height ratio (+/-Std deviation) and length variation of radial (Rd), tangential (Tg) and transversal (Tv) sections indicated.

	Height ratio H/L	Length variations ΔRd (mm)	ΔTg (mm)	ΔTv (mm)
Fresh balsa	2.67 (± 0.37)	–	–	–
Pre-immersed balsa	1.45 (± 0.17)	0 (± 0)	0 (± 0)	0 (± 0)
IP1balsa	1.41 (± 0.14)	4.25 (± 0.96)	9.75 (± 5.50)	7.75 (± 4.43)
IP2 balsa	4.45 (± 0.50)	0.25 (± 0.50)	0 (± 0)	0 (± 0)
IP3 balsa	1.55 (± 0.09)	0.75 (± 0.50)	0 (± 0)	0 (± 0)
Neolithic oak	6.21 (± 2)	-	-	-
IP1 Neolithic oak	0.74 (± 0.09)	13.42 (± 0.61)	13.42 (± 0.42)	8.17 (± 3.13)

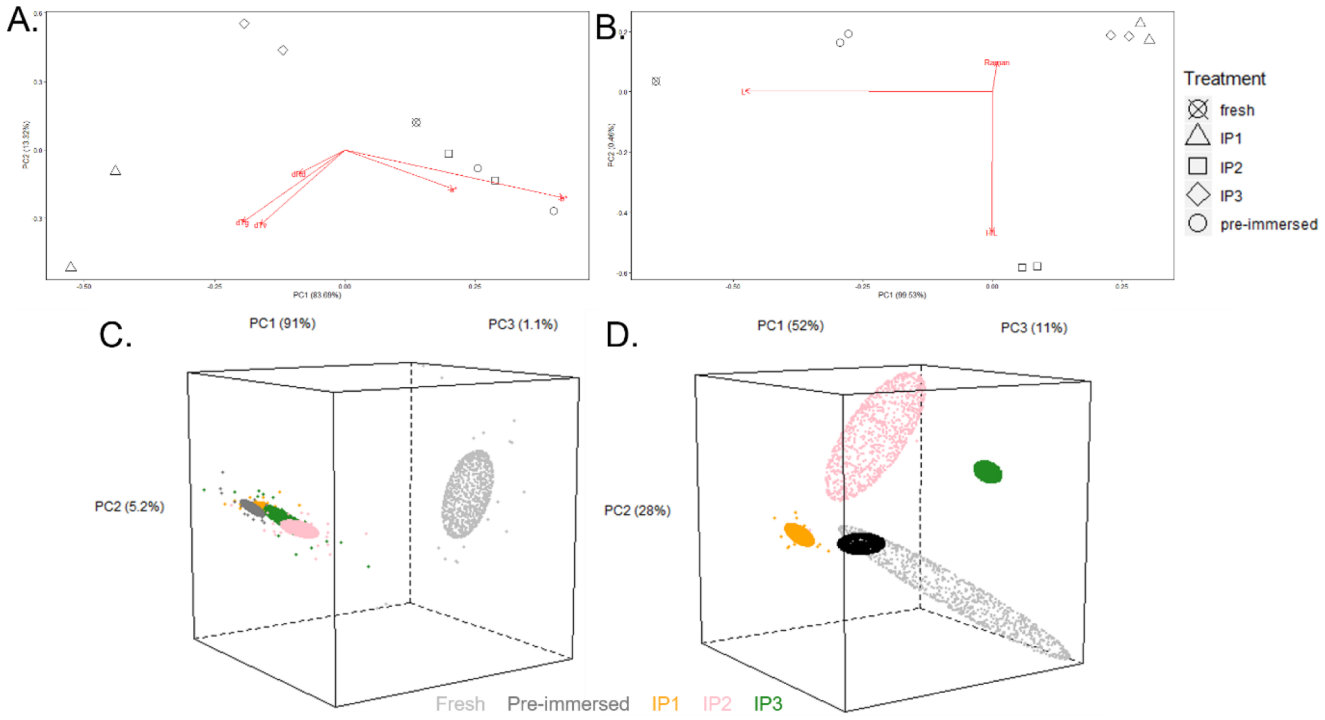

Fig. 4. PCA scores plots of the first two principal components using A. a* and b* colorimetric coordinates and shrinkage data (ΔRd, ΔTg, ΔTv) and B. brightness L*, H/L ratio and Raman data for fresh (⊗), pre-immersed (○) and impregnated (IP1 Δ, IP2 □ and IP3 ◊) balsa samples. C. 3D plot of ATR-FTIR spectra collected at LATHEMA of fresh (rip), water pre-immersed (rIP), IP1 (RIP1), IP2 (RIP2) and IP3 (RIP3) samples. D. 3D plot of ATR-FTIR spectra collected at Arc'Antique of fresh, water pre-immersed, IP1, IP2 and IP3 samples.

appearance, wood degradation and compounds identification. IP1 and IP3 samples displayed a dark hue while IP2 samples presented a brownish one. Iron oxides were identified on IP2 samples contrary to the two other protocols where iron sulfides were detected. In addition, both laboratories observed a lignin degradation for IP2 and holocellulose decay for IP1 and IP3. The Round Robin test demonstrated the reproducibility of the selected protocols on wood samples. The production of model archaeological wood samples can be implemented by any laboratory for different conservation-restoration purposes.

3.6. PCA analyses

All data obtained from the different analytical measurements were then compiled with Rstudio software and analyzed through PCA. First, the values of a*, b* and shrinkage variation were compiled together (Fig. 4 A). On this score plot, three clusters can be observed: a cluster gathering data of IP3, a second cluster gathering data of IP1, and the last cluster gathering data for IP2, t0 with and without water pre-immersion. Loadings lines (red arrows) indicate which variables have the largest effect on each principal component (PC). Colorimetric coordinates have a positive loading on PC1 for fresh (t0_dry), pre-immersed (t0-imm) and IP2 balsa samples. Shrinkage values have a negative loading on PC1 and PC2 especially for IP1 samples.

The data for brightness (L*), H/L ratio and Raman spectra (iron sulfides detected) were compiled and analyzed (Fig. 4 B). Four clusters may be distinguished. Two of them only contained data for t0 samples, gathering along the L* loading. Data for IP2 clustered along the H/L loading while data for IP1 and IP3 clustered along the Raman loading. Only Raman has a slight positive loading on both PCs as the loading is not equal to zero, contrary to L* and H/L loadings.

Moreover, PCA analysis was carried out on the ATR-FTIR spectra. From data obtained at the University of Neuchâtel (LATHEMA), two clusters were observed from the compiled data (Fig. 4 C.). The first one comprised only fresh balsa samples, while the second one gathered immersed and impregnated samples. In this second cluster, an overlapping of confident ellipses of immersed balsa and IP1 samples was observed. The IP3 confident ellipse overlapped with ellipses of IP1 and IP2. However, IP1 and IP2 samples did not present overlapping. The Arc'Antique laboratory collected dataset illustrated a clustering of fresh and immersed samples with their confident ellipses overlapping (Fig. 4 D). IP1 samples gathered close to fresh and immersed samples, but no overlapping was observed. IP2 and IP3 samples clustered farther away, with no overlapping among them or the other clusters.

The loadings plot informed of bands that can be used to differentiate the PCs. The most influential frequencies were identified in the range 3300–3350 cm^{-1} and 1030–1040 cm^{-1} for both datasets. The band at 1034 cm^{-1} is assigned to C—O stretching in holocellulose. PCs is then mainly influenced by the vibrational bands of holocellulose content of wood samples and so influenced by the degradation state of the wood.

4. Discussion

4.1. Under vacuum water pre-immersion

Particular attention was paid to the water pre-immersion step. The pre-treatment was performed to enhance the degradation of the wood samples and to model the decay grade of waterlogged archaeological wood artefacts. Indeed, the ATR-FTIR spectra, after a one-week immersion in water under vacuum, showed a shoulder at 897 cm^{-1} that was better defined. This band suggests that cellulose was affected by this pretreatment. Moreover, a shoulder at 1203 cm^{-1} also indicated an in-plane deformation of the holocellulose content [17]. These observations suggest that a water pre-immersion under vacuum step would enhance wood degradation and especially the carbohydrates content. Even though literature reported that water immersion did not affect the mechanical properties of wood, the concomitant application of vacuum may contribute to altering such properties for fresh wood [35]. The water-immersion spectrum also presented a broad band at 1650 cm^{-1} assigned to the deformation of H—O—H adsorbed water. This indicates that water was adsorbed on the wood surface. The

decreased H/L ratio is observed when a water pre-immersion step under vaccum is applied (Table 2). A diminution of the ratio implied a degradation of the holocellulose and the carbohydrates content; thus demonstrate the success of water pre-immersion under vacuum to model the degradation and state of waterlogged archaeological wood. Further investigation is necessary in order to take into account some factors that may confirm these results, such as a different moisture content between samples.

However, comparing the ratios of immersed balsa and Neolithic oak demonstrated an important difference. The immersed balsa samples have a H/L ratio of 1.45 (± 0.31) while for Neolithic oak ratio reaches 6.21 (± 2). The two different wood species may contribute to the differing ratios. Balsa and oak woods do not have same the composition, so their reactivity towards their environment may differ. A more important parameter would be degradation over time. The Neolithic oak was buried in lake sediments for centuries, where the bacterial decay slowly occurred and could reach deeper parts on the wood. For our samples, the wood was immersed only one week, which is a relatively short time compared to waterlogged wood objects. Deeper investigations would be performed to ascertain the balsa wood degradation.

Waterlogged archaeological wood artefacts may look intact while they remain wet and/or in their burial environment. Nevertheless, bacterial degradation in this environment weakened the structure. Hydrogen sulfide ions HS^- are produced during burial time and two main reactions occur. The first one involves a nucleophilic reaction of the activated double bond of lignin compounds. HS^- reacts with lignin compounds leading to the decomposition of the lignin molecules and formation of organosulfur compounds in lignin rich areas. In the second process, HS^- interacts with the iron ions present inside the wooden artefact to form iron sulfides. These compounds are produced in the bacterially degraded layer of the wood, where iron ions previously penetrated [9]. In this case, FeS_x compounds accumulated in cellulosic layers. Cellulose is the main component of wood. When the cellulosic layers are mostly decayed, the FeS_x compounds then attached to the amorphous cellulose formed by SRB. In real waterlogged wood artefacts, the presence of Fe/S species accumulated within porous wood timber on the amorphous cellulose content. This degradation is due to the presence of sulfate and SRB in the environment.

After recovery the modification of the environmental conditions results in different chemical compounds accumulated within the waterlogged wood artefacts. Oxidation of iron sulfides leads to the formation of iron oxides, iron sulfates and to sulfuric acid. FeS_x compounds produced expand in volume when environmental conditions change (higher oxygen concentration, different relative humidity). The higher molar volume of the compounds induces the cells to collapse where FeS_x attaches.

Simultaneously, the acid produced throughout this process results in acid hydrolysis of the cellulose and reduces the artefact's stability. The pH of a wood substrate can drop until a value of 3.5, and this decrease of pH allows the reaction of sulfur oxidation to continue [7].

Lignin degradation may also occur through the Fenton reaction. As radicals form, they enhance the reaction leading to slow continual decomposition of lignin (lignin is already weakened by nucleophilic reaction with HS^- during burial time) [36]. Additionally, if ferrous iron is present in the samples, then iron ions and radicals can create a cycle allowing the Fenton reaction to continue.

The holocellulose degradation induced during the water pre-immersion treatment was assessed in real waterlogged archaeological wood samples. No Fe/S species contamination was found; thus, the results were not due to acidic hydrolysis or the Fenton reaction related with the presence of such species. The results suggest that the primary cause enhancing degradation is the vacuum applied during the water pre-immersion period.

4.2. IP1

4.2.1. Fresh balsa samples

IP1 samples displayed a dark color on their surface similar to that described in literature for waterlogged archaeological wood [3]. This result suggests that the IP1 protocol confirms the criteria of appearance set in our modeling. In addition, the sample's core was also dark, indicating that the impregnation solution effectively penetrated the wood vessels. The dark hue of the samples is hypothesized to be due to the contamination of iron sulfides because balsa wood has a low tannin content, and iron-tannin complexes are unlikely to be formed [37]. If the contamination seemed homogeneous visually (low standard deviation), Raman spectroscopy suggested that the core was not as contaminated. Indeed, Raman analyses identified iron sulfide compounds, mainly partially oxidized mackinawite ($Fe_{1-x}S$) and greigite (Fe_3S_4) on the wood surface as well as within the first millimeters of the wood substrate only. Balsa being very porous wood, the iron sulfides formed during the impregnation protocol could accumulate within the wood structure such as described for waterlogged archaeological wood samples.

In addition, ATR-FTIR spectroscopy confirmed wood degradation. The intensity of peaks at 1737, 1374, 1233 and 1128 cm^{-1}, attributed to polysaccharides content, decreased [3,23]. This observation proved the degradation of carbohydrates content within wood. In past studies, waterlogged archaeological wood showed that cellulose and hemicellulose were the main wood fractions affected by the bacterial degradation during burial and post-excavation due to acid hydrolysis and exposure to oxygen upon recovery [9,38]. The visible 1233 cm^{-1} band is not described in literature, except as a shift of 1227 cm^{-1} band [39]. This band could result from overtone between 1217 and 1226 cm^{-1} bands assigned to C—O stretching vibration in guaiacyl units (a component of lignin) and C—H and C—O wagging mode in cellulose and xylan (from hemicellulose), respectively [17,23,33]. As both band intensities assigned to lignin (1506 cm^{-1}) and holocellulose (1158 cm^{-1}) decreased after IP1, we supposed that lignin content was also slightly degraded during impregnation. Lignin degradation can occur through the Fenton reaction. When radicals form, they enhance the reaction resulting in slow lignin decomposition [39]. Ferrous iron present in the samples could allow the Fenton reaction to continue by creating a cycle where ferric iron ions and radicals are produced. The calculated H/L ratio showed a diminution after IP1, suggesting that the carbohydrates content was more affected than lignin content. If a Fenton reaction occurs, then its impact on the wood substrate is less important than the alteration of carbohydrates. After oven-dried, the samples collapsed and shrank in three sections (radial, tangential and transversal). This collapse suggested a loss of mechanical strength of the samples, as observed on real objects [9,35]. A shrinkage of 20 to 50% was observed and is comparable to values obtained from waterlogged archaeological wood [27]. From these results, the impact of IP1 on wood could be compared with wood degradation occurring in burial environments. Compared with impregnated Neolithic oak, the shrinkage is more significant for radial cutting sections. However, the standard deviation was higher for impregnated balsa than for Neolithic oak samples. The difference in deviation may be due to the initial wood structure. Indeed, Neolithic oak was already decayed and its structure more fragile. Moreover the degradation within the wood is more homogeneous within Neolithic oak than impregnated fresh balsa, explaining why the shrinkage was more constant on Neolithic oak.

Some aspects of the results remain unclear and require additional assessment. The observation of FeS proved the feasibility of forming iron sulfides with IP1; however the penetration depth could be optimized. The fact that partially oxidized mackinawite was identified showed that the formed compounds were not stable. $Fe_{1-x}S$ formation may have occurred during the impregnation protocol or resulted from the oxidation of mackinawite afterwards. Indeed, mackinawite is a stable compound in an anoxic environment, but once exposed to

oxygen, it oxidizes quickly [4]. Depending on the concentrations of O_2 and/or H_2S, humidity, pH and temperature, FeS oxidizes first with iron (II) ions turning into iron (III) ions inside the crystalline structure leading to the oxidize phase $Fe_{1-x}S$ [20]. If further oxidation occurs, Rickard and Luther [40,41] and Bourdoiseau et al. [21,42] document the formation of greigite as an intermediate compound. Despite the careful attention given to avoid oxidation, this is a potential explanation of the results of the IP1 study. Impregnated samples were wrapped with a plastic film, placed in plastic bags, and stored at 4 °C in deaerated deionized water. The manipulation necessary to achieve the different analyses exposed them to room temperature and different relative humidity that may accelerate the oxidation of mackinawite.

Unintentional oxidation would also explain the observed wood degradation. As described in literature, iron ions can catalyse sulfur compounds oxidation but also the degradation of cellulose. Though, it appeared that after a one-week pre-immersion in water under vacuum, balsa wood was already partially degraded (Section 4.1.). The H/L ratio values obtained for pre-immersed and IP1 samples were similar (1.45 versus 1.41), aiding in the suggestion that water pre-immersion, not chemicals used during impregnation, primarily caused the cellulose degradation in samples. A deeper investigation regarding this water pre-immersion step should be performed to understand better the degradation mechanisms occurring with water on wooden substrates. On real waterlogged wood objects, the bacteria degraded the wood from the cell lumen to the secondary wall where the iron sulfides accumulated. Microscopic observations of thin sections showed that only balsa wall cells were visible, as balsa is a very porous wood, but the compounds were not observed. Assessment with a scanning electron microscopy will be carried out to investigate the cell walls and how the iron and sulfur species interact with the wood matrix.

It should be noted that pyrite (FeS_2) was never detected on our samples, while it is widely documented and observed on waterlogged archaeological wood. The impregnation solution was an equimolar solution of Fe(II) and S(-II), which decreases the likelihood for pyrite forming with its ratio of Fe:S = 1:2. Optimization of the protocol could be achieved with different Fe and S concentrations allowing FeS_2 to form.

4.2.2. Neolithic oak samples

The results obtained from the application of the three impregnation protocols on fresh balsa samples suggested that IP1 was the most efficient in terms of wood degradation and iron sulfides formation. This protocol was then applied to Neolithic oak samples.

Color measurements performed after impregnation resulted in a brightness level of 25.51 (± 0.1). This value was similar to the one obtained from fresh balsa impregnated with IP1 (25.71 ± 0.8). These results proved that the IP1 protocol produces a similar appearance, whatever the wood type. However, the color observed in analogues is not identical to the coloration of real waterlogged archaeological wood [43].

Raman spectroscopy applied to Neolithic oak wood before the impregnation protocol showed no reduced sulfur species. Thus, the Neolithic wood samples were not contaminated with such species. The application of an impregnation protocol leads to the formation of iron sulfides as for fresh balsa wood. This demonstrated that the formation of Fe/S species occurred independently of the wood type (balsa or oak in our case). In contrast to the balsa samples, fresh oak contains tannin [43,44] which have the potential to react with iron to form Fe-tannin complexes [45,46]. However, no Fe-tannin compounds were identified during the Raman analyses [47,48]. The absence of tannin complexes can be attributed to the advanced state of degradation of Neolithic oak wood. After an extended burial time, several wood components, such as tannin, decay. Thus, the eventual formation of Fe-tannin complexes in the presence of iron is avoided.

The additional analyses carried out through ATR-FTIR spectroscopy indicated that the H/L ratios obtained for fresh balsa and Neolithic oak decreased after impregnation, suggesting a carbohydrates degradation occurred in both cases. The decrease was surprisingly more important for Neolithic oak. This result was not expected. The extended burial period for Neolithic wood typically results in more extensive holocellulose degradation than observed pre-treatment. The decrease of the ratio suggests that (1) the archaeological samples did not experience the amount of carbohydrate degradation anticipated, and (2) the holocellulose was further degraded during IP1 protocols. This observation is in congruence with the results discussed in Section 4.2. While balsa and oak have different chemical compositions, densities and structures, the impregnation protocol leads to wood degradation and the formation of sulfur species. A study on fresh oak artificially degraded then impregnated with IP1 should be carried out to verify these findings further and account for innate differences in wood species.

As discussed in Section 4.2, the presence of partially oxidized mackinawite ($Fe_{1-x}S$) suggested that IP1 initiates the formation of intermediary iron phases that are not as stable as other compounds like mackinawite or greigite. The oxidation of the compounds formed may occur due to the storage of samples in deaerated water for a couple of days before being characterized. An optimized analytical protocol should help ascertain the different phases formed and better understand the possible wood degradation process occurring.

4.3. IP2

IP2 treated samples only presented a homogeneous brown hue of the surface after impregnation for 60 days; however the solution did not penetrate deeply into the core of the samples. Two centimeters is the effective degradation depth observed on the *Vasa* or the *Mary Rose* warships [9]. Given documented degradation depths, the results of IP2 protocol would not be representative of degradation occurring on real waterlogged wood even if applied on larger samples ($3 \times 3 \times 3$ cm^3 for instance). Moreover, the iron and sulfur species formed during impregnation were iron oxides, lepidocrocite (γ-FeOOH), and not iron sulfides as desired. This corrosion product gave a brownish hue to the wood quite different from the darker, nearly black, hue usually observed on waterlogged wood artefacts. In this solution, the sulfur source was sodium sulfate Na_2SO_4 and not sulfide salt. Therefore, iron sulfates, such as melanterite ($FeSO_4.7H_2O$), were expected to form. The corroded terrestrial nails used in IP2 protocol were also analyzed by Raman spectroscopy to characterize the composition of the corrosion layer. Lepidocrocite was detected in the corrosion layer of the terrestrial nails. It can be postulated that the nails corrosion layer partly solubilized and contaminated the wood samples. Even if iron (III) phases present a very low solubility in water, the slightly acidic (pH 6) IP2 solution may have allowed partial solubilization throughout the 60 days of impregnation [44]. Compounds observed on IP2 samples are reported in literature as oxidation compounds once the waterlogged archaeological wood samples have been exposed to atmospheric conditions. As explained in Section 4.1., oxidation compounds have a larger volume than iron sulfides, which lead to cracks within the wood cells.

The ATR-FTIR analyses suggest that the wood content mainly degraded in IP2 was lignin. As observed by Franceschi et al. [45], the artificial seawater and the presence of metal affected the wood's composition and induced degradation of its content. Although Franceschi et al. [45] observed a diminution of the cellulosic content, lignin degradation was predominantly observed in this study. The use of balsa instead of oak wood may explain in part why lignin was degraded while carbohydrates content was not degraded during IP2 treatment, given the differing wood compositions and densities of the two wood species. In particular the intensity decrease of 1595 cm^{-1} vibrational band indicated the modification of the aromatic skeleton of lignin [23]. In addition, the 1737 cm^{-1} band intensity remained identical before and after the IP2 application so the polysaccharides content was not affected [46].

Above, we concluded that carbohydrates content was affected and degraded mainly during the water pre-immersion step rather than during IP1. With IP2, an increase of the H/L ratio was observed and would suggest that the lignin content was affected and mainly degraded in the treatment process. This result may be caused by the chemical used during impregnation or by the impregnation duration. Studies have demonstrated that organic substances are oxidized concurrently during ferrous-ferric transformation in aqueous media, and delignification occurs when wood was exposed to rusting iron [47]. A labile metal ion-molecular complex is formed and causes the formation of free radicals that degrade organic matter, such as wood. The well-documented Fenton reaction comes out from this degradation by free radicals and would explain the lignin degradation and the high H/L ratio observed after IP2 [10,17]. In addition, the structure of the samples remained identical after oven-dried which verifies that no physical properties were affected by this treatment contrary to waterlogged wood artefacts in burial environments. Cellulose and hemicellulose, present within the cells, were not decayed enough to lead to a loss of strength or cause the collapse of the entire sample.

These results showed the failure of IP2 to model waterlogged archaeological wood through the formation of iron sulfides and the degree of wood degradation. This impregnation protocol should be disregarded from further contention.

4.4. IP3

IP3 samples developed a very similar appearance to the IP1 samples. Their colorimetric coordinates were close on both CIELab plots (Fig. 2 B) which suggests that similar compounds have formed during the impregnation. However, spectroscopies analyses showed that IP3 did not give the same results as for IP1.

For instance, sulfur was the main compound identified with minor proportions of greigite. A hypothesis could be that the preferential precipitation of mineral sulfur is due to a higher concentration of sulfides with respect to iron ions. However, elemental sulfur was not reported to give black a hue but more yellowish spots [1]. The few iron sulfides detected would then give the dark color. While the impregnation policy to maintain a neutral solution may have interfered with Fe/S species formation and prevented the precipitation of iron sulfides. As for IP1, reduced sulfur species may have accumulated within the porous wood timbers.

Complementary ATR-FTIR spectra display similar bands before and after IP3. Alternatively, IP2 spectra seemed to indicate that lignin content was more affected with a decrease of the relative intensity of the 1595 cm^{-1} band, assigned to aromatic skeleton of lignin. The calculated H/L ratio showed a decrease compared to fresh balsa wood, while the ratio after IP3 was similar to the ones of water pre-immersion and IP1 balsa wood. The ratio suggests that neither lignin nor the amount of carbohydrates was degraded after IP3. If carbohydrates content was predominantly degraded, acidic hydrolysis could be occurring as hydrochloric acid (HCl) was used to maintain a neutral pH. It is unlikely that HCl will degrade the holocellulose. Ferrous iron was also added to the sulfide solution to precipitate iron sulfides. The presence of ferrous iron could induce a Fenton reaction with free radicals. However, given the ratio obtained, it is doubtful that this reaction occurs as iron compounds were not formed during the impregnation protocol and remained mostly in solution. All these observations suggested that IP3 did not model the degradation and structure of waterlogged archaeological wood samples.

Notably, contrary to the spectra recorded after IP1 and IP2 impregnation protocols, two weak bands could be observed at 1537 and 1550 cm^{-1}. These vibrational bands are not reported in literature. The spectra of fresh or archaeological wood reported in other studies never display these bands, nor do they correspond to characteristics vibrational bands of sulfur [17,33,39]. They may correspond to the aromatic skeletal vibration of lignin that has bands at 1506 and 1595 cm^{-1}. Further investigations should be conducted to determine the impact of this impregnation protocol with regards to wood degradation and the unidentifiable bands observed.

4.5. Validation by chemometrics

The statistic applied to our data validated which treatment was the most accurate of modeling the waterlogged archaeological wood available.

According to our previous observations, PCA analyses did validated the effect of water pre-immersion on the wood samples. On the first score plot, non-water immersed balsa and IP2 samples gathered, which suggests that water immersion step was not significant. On the second score plot, water pre-immersed samples did not cluster with the non-immersed samples nor with the impregnated samples(Figs.4. A and 4. B). Instead, they formed a distinct cluster along the L* loading. It can be concluded that water pre-immersion step influenced the appearance of wood samples. While the IP2 samples that clustered along H/L loading, the water pre-immersed samples gathered far from them. This split proved that the ATR-FTIR spectra recorded and ratio calculated on water pre-immersed samples were different from all other samples. Thus, this information verified that the water pre-immersion affected the wood composition. Future experimentation should be done to validate the use of vacuum by comparing results from water pre-immersion under and without vacuum. If ATR-FTIR data are separated by PCA, vacuum will then be an important parameter in modelling waterlogged archaeological wood.

Chemometrics also validate that IP1 was the most suitable protocol based on the parameters of the waterlogged wood available. On both score plots, IP2 samples clustered far from IP1 and IP3 samples verifying that this protocol differed from the two others. Chemometrics then eliminated the IP2 protocol from contention. Furthermore, no significant difference between IP1 and IP3 samples could be observed on the score plot with L*, H/L and Raman loadings (Fig. 4 B). IP1 was determined as the best protocol due to the high degree of wood shrinkage obtained after impregnation. All samples gathered on the first score plot suggesting they were similar. On the second score plot (Fig. 4 A), IP1 samples gathered along the shrinkage loadings while the IP3 gathered far from them. As we described in the results Section 3, IP1 led to a higher and more significant collapse of the wood structure. The IP1 protocol affects the wood internally more than IP3. This observation also supports the supposition that both water pre-immersion and IP1 enhanced wood degradation, by increasing damages on the internal structure.

A deeper investigation of the ATR-FTIR spectra was performed. The firsts observations showed similar results for the Round Robin test. Nevertheless, differences were displayed when PCA was applied on the datasets.

For LATHEMA, two main clusters were observed during the PCA analysis, gathering fresh balsa and water pre-immersed and impregnated samples, respectively. In this second cluster, the loading plot showed that the bands at 1274, 1366 and 1732 cm^{-1} were the less influenced frequency variables. All these bands are assigned to hemicellulose, in particular xylan. However, lignin and holocellulose did contribute to the PCs with the most influenced variables bands at 1034 cm^{-1} and at 1059 cm^{-1}, which are assigned to these wood components. Both these vibrational bands contribute equally to the formation and distinction of the cluster between the impregnation protocols.

One-way ANOVA analysis was performed with the PCs obtained from PCA. On the plot, fresh and water pre-immersed balsa samples gathered and were significantly distant from the impregnated samples ($F(1,3) = 601.6$, $p < 0.001$). In addition, one-way ANOVA was performed on the values of ATR-FTIR H/L ratios. Results obtained showed a significant difference among the two clusters obtained (fresh and IP2 balsa against pre-immersed, IP1 and IP3 balsa) with an F value of 23.5

and a p-value $p < 0.001$.

For Arc'Antique, fresh and immersed balsa samples clustered and overlapped suggesting that no clear distinction can be made between these two sets of samples. However, no overlapping was observed between impregnated samples and fresh-immersed samples cluster. The application of IP1, IP2 and IP3 led to chemical changes as the PCA analysis showed. The IP1's cluster was closer to the immersed samples while IP3's cluster was the farther. Surprisingly, even though PCA plots for Arc'Antique and LATHEMA data did not present similar results, the same variables were used for both of them to synthesize the data. The wavenumbers in the range 1030-1050 cm^{-1} are the most important to differentiate data and to understand the obtained results. One-way ANOVA performed also showed a significance among the data with $F = 56.3$ and $p < 0.001$.

Differences in the dataset can come from manipulations and the instrument used for measurements. Further analyses should be carried out to have a better understanding of the effects of water pre-immersion under vacuum and artificial impregnation have on the wood structure.

5. Conclusions

This study presented the modeling of waterlogged archaeological wood from fresh balsa wood. The preparation of model samples from fresh wood by artificial degradation can be a promising way to test novel extraction methods for the conservation of waterlogged archaeological wood in the future. Optimization of model sample preparation would allow any laboratory to have a homogeneous set of waterlogged wood samples with similar characteristics. New extraction or consolidation treatments could then be studied on these sacrificial samples. The structure of the sample and the performances of the treatment could be deeply investigated. In particular, the key factors allowing to simulate degraded waterlogged wood were individuated. Due to the application of statistical methods, IP1 was determined and validated as the most suitable impregnation protocol for the artificial contamination and degradation of fresh balsa wood. A water pre-immersion followed by impregnation in an equimolar solution of Fe(II) and S(-II) under vacuum appears essential to form iron sulfides such as mackinawite properly as well as to degrade wood carbohydrates content effectively. Pyrite (FeS_2) was not detected in our study. Further experiments should be performed to optimize the current protocol with different chemicals and under different conditions, such as weathering samples in a climatic chamber or using specific wood-degrading fungal strains. Moreover, even if this study showed the feasibility and efficiency of IP1 to reproduce some of the characteristics of degraded waterlogged wood, modeling will continue to be improved upon for wood species frequently encountered in waterlogged wood artefacts, such as oak and pine wood.

CRediT authorship contribution statement

Mathilde Monachon: Software, Validation, Formal analysis, Investigation, Data curation, Writing - original draft, Writing - review & editing. **Magdalena Albelda-Berenguer:** Investigation. **Charlène Pelé:** Investigation, Validation. **Emilie Cornet:** Investigation. **Elodie Guilminot:** Validation. **Céline Rémazeilles:** Validation. **Edith Joseph:** Conceptualization, Methodology, Validation, Writing - original draft, Writing - review & editing, Supervision, Project administration, Funding acquisition.

Declaration of Competing Interest

None.

Acknowledgments

The authors want to acknowledge the Swiss National Science Foundation for the Professorship Grant PP00P2_163653/1, 2016–2020. The authors also acknowledge the HES-SO of Fribourg for the access to the Raman microscope, Benedetto Pizzo and Nicola Macchioni from IVALSA, Italy and Dawa Chen (China) for their help and contribution regarding the understanding of the mechanism of wood degradation. The authors acknowledge Sarah M James for copy-editing process.

References

[1] K.M. Wetherall, et al., Sulfur and iron speciation in recently recovered timbers of the Mary Rose revealed via X-ray absorption spectroscopy, J. Archaeol. Sci. 35 (5) (2008) 1317–1328.
[2] C. Pelé, E. Guilminot, S. Labroche, G. Lemoine, G. Baron, Iron removal from waterlogged wood : extraction by electrophoresis and chemical treatments, Stud. Conserv. 0 (0) (2013) 1–17.
[3] G. Almkvist, I. Persson, Extraction of iron compounds from wood from the Vasa, Holzforschung 60 (6) (2006) 678–684.
[4] C. Rémazeilles, et al., Microbiologically influenced corrosion of archaeological artefacts: characterisation of iron(II) sulfides by Raman spectroscopy, J. Raman Spectrosc. 41 (11) (2010) 1425–1433.
[5] C. Rémazeilles, F. Lévêque, E. Conforto, L. Meunier, P. Refait, Contribution of magnetic measurement methods to the analysis of iron sulfides in archaeological waterlogged wood-iron assemblies, Microchem. J. 148 (2019) 10–20. April.
[6] C. Rémazeilles, et al., Studies in conservation post-treatment study of iron/sulfur-containing compounds in the wreck of Lyon Saint-Georges 4 (second century ACE), Stud. Conserv. 0 (0) (2019) 1–9.
[7] M. Sandström, F. Jalilehvand, I. Persson, U. Gelius, P. Frank, I. Hall-Roth, Deterioration of the seventeenth-century warship Vasa by internal formation of sulphuric acid, Nature 415 (6874) (2002) 893–897.
[8] J. Preston, A.D. Smith, E.J. Schofield, A.V. Chadwick, M.A. Jones, J.E.M. Watts, The effects of Mary Rose conservation treatment on iron oxidation processes and microbial communities contributing to acid production in marine archaeological timbers, PLoS One 9 (2) (2014).
[9] Y. Fors, M. Sandström, Sulfur and iron in shipwrecks cause conservation concerns, Chem. Soc. Rev. 35 (5) (2006) 399–415.
[10] Y. Fors, T. Nilsson, E.D. Risberg, M. Sandström, P. Torssander, Sulfur accumulation in pinewood (Pinus sylvestris) induced by bacteria in a simulated seabed environment: implications for marine archaeological wood and fossil fuels, Int. Biodeterior. Biodegrad. 62 (4) (2008) 336–347.
[11] M. Sandström, Y. Fors, F. Jalilehvand, E. Damian, U. Gelius, Analyses of sulfur and iron in marine-archaeological wood, Proc. 9th ICOM Gr. Wet Org. Archaeol. Mater. Conf. Copenhagen, 2004, pp. 181–202 2005.
[12] Y. Fors, V. Richards, The effects of the ammonia neutralizing treatment on marine archaeological Vasa wood, Stud. Conserv. 55 (1) (2010) 41–54.
[13] P. Baglioni, E. Carretti, D. Chelazzi, Nanomaterials in art conservation, Nat. Nanotechnol. 10 (4) (2015) 287.
[14] A. Tahira, W. Howard, E.R. Pennington, A. Kennedy, Mechanical strength studies on degraded waterlogged wood treated with sugars, Stud. Conserv. 62 (4) (2017) 223–228.
[15] M. Broda, B. Mazela, K. Radka, Methyltrimethoxysilane as a stabilising agent for archaeological waterlogged wood differing in the degree of degradation, J. Cult. Herit. xx (Jun. 2018) no. x.
[16] M. Albelda Berenguer, et al., Biological oxidation of sulfur compounds in artificially degraded wood, Int. Biodeterior. Biodegradation. (Jul. 2018) June.
[17] G. Almkvist, S. Norbakhsh, I. Bjurhager, K. Varmuza, Prediction of tensile strength in iron-contaminated archaeological wood by FT-IR spectroscopy-a study of degradation in recent oak and Vasa oak, Holzforschung 70 (9) (2016) 855–865.
[18] S. Norbakhsh, I. Bjurhager, G. Almkvist, Impact of iron (II) and oxygen on degradation of oak - modeling of the Vasa wood, Holzforschung 68 (6) (1974) 649–655.
[19] M. Borrega, P. Ahvenaine, R. Serimaa, L. Gibson, Composition and structure of balsa (Ochroma pyramidale) wood, Wood Sci. Technol. 49 (2015) 403–420.
[20] C. Rémazeilles, K. Tran, E. Guilminot, E. Conforto, P. Refait, Study of Fe(II) sulphides in waterlogged archaeological wood, Stud. Conserv. 58 (4) (2013) 297–307.
[21] J.A. Bourdoiseau, M. Jeannin, R. Sabot, C. Rémazeilles, P. Refait, Characterisation of mackinawite by Raman spectroscopy: effects of crystallisation, drying and oxidation, Corros. Sci. 50 (11) (2008) 3247–3255.
[22] R.M. Cornell, U. Schwertmann, The Iron Oxides: Structure, Properties, Reactions, Occurrences and Uses, John Wiley & Sons, 2003.
[23] B. Pizzo, E. Pecoraro, A. Alves, N. Macchioni, J.C. Rodrigues, Quantitative evaluation by attenuated total reflectance infrared (ATR-FTIR) spectroscopy of the chemical composition of decayed wood preserved in waterlogged conditions, Talanta 131 (2015) 14–20.
[24] K.K. Pandey, A.J. Pitman, FTIR studies of the changes in wood chemistry following decay by brown-rot and white-rot fungi, Int. Biodeterior. Biodegrad. 52 (3) (2003) 151–160.
[25] I. Dobrică, P. Bugheanu, I. Stănculescu, C. Ponta, FT-IR spectral data of wood used in Romanian, Analele Univ. din Bucuresti I (2008) 33–37.
[26] K.K. Pandey, H.C. Nagveni, Rapid characterisation of brown and white rot degraded chir pine and rubberwood by FTIR spectroscopy, Holz als Roh- und Werkst. 65 (6) (Nov. 2007) 477–481.
[27] N. Macchioni, B. Pizzo, C. Capretti, E. Pecoraro, L. Sozzi, S. Lazzeri, New wooden archaeological finds from Herculaneum: the state of preservation and hypothesis of

consolidation of the material from the house of the relief of telephus, Archaeometry 58 (6) (2016) 1024–1037.
[28] N. Macchioni, B. Pizzo, C. Capretti, An investigation into preservation of wood from Venice foundations, Constr. Build. Mater. 111 (2016) 652–661 March.
[29] J.A. Bourdoiseau, M. Jeannin, C. Rémazeilles, R. Sabot, P. Refait, The transformation of mackinawite into greigite studied by Raman spectroscopy, J. Raman Spectrosc. 42 (3) (2011) 496–504.
[30] B. Meyer, Elemental sulfur, Chem. Rev. 76 (3) (1976) 367–388.
[31] M. Bouchard, D.C. Smith, Catalogue of 45 reference Raman spectra of minerals concerning research in art history or archaeology, especially on corroded metals and coloured glass, Spectrochim. Acta Part A Mol. Biomol. Spectrosc. 59 (10) (2003) 2247–2266.
[32] C.M.A. McQueen, et al., New insights into the degradation processes and influence of the conservation treatment in alum-treated wood from the Oseberg collection, Microchem. J. 132 (2017) 119–129.
[33] B. Pizzo, E. Pecoraro, N. Macchioni, A new method to quantitatively evaluate the chemical composition of waterlogged wood by means of attenuated total reflectance fourier transform infrared (ATR FT-IR) measurements carried out on wet material, Appl. Spectrosc. 67 (5) (2013) 553–562.
[34] S. Durmaz, Ö. Özgenç, Vibrational Spectroscopy Examination of the chemical changes in spruce wood degraded by brown-rot fungi using FT-IR and FT-Raman spectroscopy, Vib. Spectrosc. 85 (2016) 202–207.
[35] S. Norbakhsh, I. Bjurhager, G. Almkvist, Mimicking of the strength loss in the Vasa : model experiments with iron-impregnated recent oak, Holzforschung 67 (6) (2013) 707–714.
[36] S. Andrea and A. Haz, "Degradation of lignin via Fenton reaction," no. June 2015, 2014.
[37] G.J. Ritter, L.C. Fleck, Chemistry of wood, J. Ind. Eng. Chem. 14 (11) (1922) 1050–1053.
[38] I. Bjurhager, et al., State of degradation in archeological oak from the 17th century vasa ship: substantial strength loss correlates with reduction in (holo)cellulose molecular weight, Biomacromolecules 13 (8) (2012) 2521–2527.
[39] K. K. Pandey and K. S. Theagar, "Analysis of wood surfaces and ground wood by diffuse reflectance (DRIFT) and photoacoustic (PAS) fourier transform infrared spectroscopic techniques," 1997.
[40] D. Rickard, G.W. Luther, Kinetics of pyrite formation by the H2S oxidation of iron (II) monosulfide in aqueous solutions between 25 and 125 °C: the mechanism, Geochim. Cosmochim. Acta 61 (1) (1997) 135–147.
[41] D. Rickard, G.W. Luther, Chemistry of iron sulfides, Chem. Rev. 107 (2007) 514–562 2.
[42] J.-A. Bourdoiseau, M. Jeannin, C. Rémazeilles, R. Sabot, P. Refait, The transformation of mackinawite into greigite studied by Raman spectroscopy, J. Raman Spectrosc. 42 (3) (Mar. 2011) 496–504.
[43] C. Rémazeilles, et al., Studies in conservation post-treatment study of iron/sulfur-containing compounds in the wreck of Lyon Saint-Georges 4 (second century ACE), Stud. Conserv. 0 (0) (2019) 1–9.
[44] U. Schwertmann, Solubility and dissolution of iron oxides, Iron Nutr. Interact. Plants (1991) 3–27.
[45] E. Franceschi, I. Cascone, D. Nole, Thermal, XRD and spectrophotometric study on artificially degraded woods, J. Therm. Anal. Calorim. 91 (1) (2008) 119–123.
[46] M. Schwanninger, J.C. Rodrigues, H. Pereira, B. Hinterstoisser, Effects of short-time vibratory ball milling on the shape of FT-IR spectra of wood and cellulose, Vib. Spectrosc. 36 (2004) 23–40.
[47] J. Emery, H. Schroeder, Iron-catalyzed oxidation of wood carbohydrates*, Wood Sci. Technol. 8 (1974) 123–137.
[48] S. Vaclavkova, N. Schultz-Jensen, O.S. Jacobsen, B. Elberling, J. Aamand, Nitrate-controlled Anaerobic oxidation of pyrite by Thiobacillus cultures, Geomicrobiol. J. 32 (5) (2015) 412–419.